

Fermi National Accelerator Laboratory

FERMILAB-Pub-81/31-EXP
7180.557
(Submitted to Nucl. Instrum. Methods)

A SEGMENTED CALORIMETER FOR HIGH- P_t JET EXPERIMENTS

P. Rapp, P. Devensky, B. C. Brown, and H. Haggerty
Fermi National Accelerator Laboratory
Batavia, Illinois 60510

and

R. Abrams, F. Lopez, and D. McLeod
University of Illinois, Chicago Circle
Chicago, Illinois 60680

and

H. Strobele
University of Maryland
College Park, Maryland 20742

March 1981



A Segmented Calorimeter for High- P_t Jet Experiments

P. Rapp, P. Devensky*, B.C. Brown, H. Haggerty,
Fermilab National Accelerator
Batavia, Illinois

and

R. Abrams, F. Lopez, D. McLeod,
University of Illinois, Chicago Circle
Chicago, Illinois

and

H. Strobele†
University of Maryland

ABSTRACT

A large aperture (8' x 10') calorimeter for studying high- P_t hadronic interactions has been assembled at Fermilab. The depth is 16 radiation lengths of Pb followed by 7.5 absorption lengths of Fe. There are 280 readout channels. Approximately 20% of the detector was tested in preliminary running. The results, presented here, meet or exceed the design goals established for linearity, resolution, uniformity, granularity, electromagnetic/hadronic separation, and ease of calibration and monitoring.

*Permanent Address: Institute of Technology and Chemistry,
Sofia, Bulgaria

†Permanent Address: G.S.I., Darmstadt, West Germany

INTRODUCTION

We report here on the design, construction, and performance of a highly modularized total absorption calorimeter for use as both a high- P_t trigger and a neutral spectrometer in the multiparticle spectrometer (MPS) at Fermilab. The calorimeter replaces the previous E260 calorimeter as part of a significant upgrade of the MPS facility. The chief improvements in the new detector are a much finer granularity, with insignificant dead space, and a much greater acceptance, covering full azimuth around the 90° polar angle in the center of mass system. The simultaneous increase in size and granularity has been achieved very economically. Table 1 displays the main characteristics of the new calorimeter.

Our approach to finer granularity is to use many small modules, each one functioning as an independent calorimeter¹. We chose this approach for its promise of clean and unambiguous (x,y) localization. Design difficulties include minimizing or eliminating cracks between modules and maintaining adequate uniformity over each module.

The solution to packing the modules tightly derives from a shower counter of Atwood et al². This device (Fig. 1) is a standard Pb/Sc or Fe/Sc shower sampler with a waveshifter bar running along one edge. The blue light from the scintillator (Sc) is absorbed by the BBQ in the wavebar and isotropically

emitted as green light³. A significant fraction of this light is conducted by total internal reflection to the phototube at one end of the wavebar. Serendipitously the waveshifting technique solves the problem of matching large areas (160 in.² in our case) of scintillator output to small photocathode areas, typically 2 in.².

DESIGN

Our first tests (Spring 1978) were with modules very similar to Fig. 1. The main question concerned the nature of the basic sampling step. The answer was that 1/2" Fe followed by 1/2" acrylic scintillator gave adequate resolution. The acrylic gave only 20% of the light output of NE102, but with so much scintillator feeding one phototube that was sufficient. In dollars per photon the doped acrylic is considerably cheaper than NE102.

For our second round of tests (Fall 1978) we built a prototype of 27 modules. Longitudinally there were three sections: Pb/Sc, Fe/Sc, Fe/Sc. Each section was 3 modules high by 3 modules across; each module was 8" x 8". We tested five different dopings of acrylic scintillator and two different dopings of acrylic wavebar; the various dopings were suggested by reports from similar work at CERN^{4,5}. Our final choice of scintillator doping is 3% naphthalene, 1% PPO, and 0.025% POPOP, by weight.⁶ For wavebars we use 90 mg/l BBQ?

This prototype was also used to study the effect of three different nonuniformities: (1) The light output from one edge of a piece of scintillator depends on where the particle passes through the piece. (2) The fraction of light delivered to the tube by the wavebar depends on how far from the tube the light enters the wavebar. (3) Particles traversing the wavebar may generate a direct wavebar signal indicating an energy deposition higher than actually was the case. This last, the problem of "hotspots", is a very serious difficulty if the spectrum being measured falls steeply, as does the high- P_t production spectrum.

The third round of tests (1979) was a lengthy series of table-top experiments using Strontium 90 sources to understand and minimize these three nonuniformities. The scintillator pieces were 'hottest' near the middle of the output edge and 'cooler' toward the other three edges. By painting the back edge with white paint⁸ we boosted the signal from the back half considerably more than the signal from the front half (Fig. 2). Each piece is wrapped in aluminum foil, shiny side in. We found that by first taping 3" black photographic tape to the lower edge of the aluminum foil we could make a non-reflecting skirt around the faces near the output edge. This further lowered the front/back difference. Finally, the side/middle difference was eliminated by painting thin strips of white paint across the output edge; the middle strip (0.4") was flanked on both sides by successively thinner (0.2" and 0.1") strips at 1" intervals.

Similar techniques, white paint on the end far from the tube and black tape on the face near the tube, were used to flatten the wavebar attenuation. A #4 Wratten filter was placed between the wavebar and the tube to cut the effect of frequency-dependent absorption by the acrylic wavebar. The combined filtering, painting, and masking increases the wavebar attenuation length to $\lambda_w \sim 12m$. A Monte Carlo simulation indicates that shower resolution improves only negligibly for λ_w increasing beyond $\lambda_w \sim 5m$.

To minimize the direct particle/wavebar signal we tested wavebar samples made with ultraviolet absorber (UVA) added to the BBQ in the acrylic. The direct particle signal is assumed to be generated by γ light produced largely in the ultraviolet and shifted by the BBQ into the green. Three tests were made comparing the UVA and UVT (uv transparent) wavebars. The first showed that both are equally efficient at shifting scintillator light. The second showed that sources shining directly into UVA wavebars produce about 1/2 the signal produced similarly from UVT wavebars. The third test used a transmission spectrophotometer to measure the properties of the two wavebars. It showed that UVT wavebars shift a considerable fraction of the light from the 300-400 nm range, while the UVA wavebars shift none of this light. We estimate from these tests that the use of UVA wavebars cuts the direct particle/wavebar signal by 1/2.

During the course of these table-top tests we discovered that different pieces of scintillator produce different amounts of light, varying up to a factor 2. This is in itself a serious nonuniformity. To eliminate it we have used sources to measure the light output from each of the 8000 scintillator pieces. The light output is quantified by the direct current output of a phototube looking directly at the illuminated scintillator piece. Each piece is labeled and pieces of similar output are grouped together in one module.

CONSTRUCTION

Imagine that several modules of Fig. 1 are placed side by side. If the scintillator pieces are wrapped in aluminum foil for optical isolation there is no reason why the metal plates (Fe or Pb) need to be cut into squares. If the metal plates be 8" x 40" and supported on the ends there can be 5 abutted modules with vertical cracks no thicker than two layers of aluminum foil (1.5 mils). Such a structure, a crate, is shown in the exploded view of Fig. 3. There are 40 x 1/2" Fe plates tack-welded onto two 3/8" sidebars. The plug and bevel welds are very small as they need to supply only minimal structural strength. The notches on the sidebar extensions are for hanging 1/4" Pb plates for the upstream electromagnetic section. We tested 1/4" Pb (6% antimony) plates by marking scribe lines on 8" x 40" pieces and hanging them by 3/8" ears. After 18 months there is no sign of sag in the scribe lines.

We constructed 30 such crates, in 3 sizes: 12" x 40", 8" x 40", and 8" x 48". They are stacked as shown in Fig. 4. Vertically the crates are spaced by long rod stock pieces, 1/4" x 1/4" x 55". The rod stock pieces also serve two other purposes: they support the scintillator pieces 1/16" above the wavebars, and they optically isolate the wavebars, which lie in Alzac⁹ pans between the rod stock pieces. (Fig. 3) There are separate wavebars for the Pb and Fe sections, called respectively, EM (electromagnetic) and FH (Front Hadron). The EM wavebars are 12 3/8" long and couple to lightpipes which curve around 90° to go up or down to RCA 6342A phototubes above and below the upstream face of the stack. The FH wavebars are 42 3/8" long and couple similarly to tubes above and below the downstream face. All the photocathodes are 42" above or below beam height. Scintillator pieces sit both in front of the first Pb plate and in back of the last FE plate; they are held in place by 1/4" phenolic pieces attached to the sidebar ends. The entire stack, the EM/FH unit, sits on a motorized table which moves in x and y to provide fast beam calibration of every module. The three modules in each corner are not instrumented, leaving the 126 modules shown schematically in Fig. 5.

The BH (Back Hadron) unit is a similar but coarser stack of steel crates. There are 24 crates, each with 23 plates, each plate being 1" x 20" x 28". The 1/2" scintillator is in two sizes, 13 1/2" x 20" and 27" x 20". The corner crates are not instrumented, leaving the 28 modules shown schematically

in Fig. 6. The BH unit sits on its own motorized table; with the beam passing through the EM/FH unit hole the BH modules can be very quickly beam calibrated.

Each of the 280 lightpipes has attached to it an optic fiber which feeds BBQ-shifted laser light into the wavebar. The returning signal monitors the entire chain of wavebar/lightpipe/tube/cabling as well as both the ADC's and the trigger electronics. The laser is monitored by photodiodes and can be triggered to fire between beam spills. By correlating the monitor signal with the beam signal at the time of calibration we can establish a reference for continual monitoring.

PERFORMANCE

Fig. 7 shows the calorimeter response to five beam energies. The points are normalized to 40 GeV. The beam was essentially pions, with an electron component growing from 10% at 20 GeV to 65% at 10 GeV. At 200 GeV the response is low by 7%, which is compatible with our estimate of the longitudinal leakage. The estimate is made by extrapolating the measured 22% leakage from the EM/FH unit into the BH unit. Over the four lower energy points the detected energy diverges linearly from the beam energy. Extrapolated to zero beam energy the plot indicates a remnant detected energy of 2.5 GeV. The divergence from 'slope 1' and the resulting offset are assumed due to an offset in the beam line magnet current readback.

The hadron resolution is shown in Fig. 8. It follows the curve of $70\%/\sqrt{E}$ at higher energies and is somewhat better at lower energies.

The electron resolution (Fig. 9) was measured in the high resolution beam at the Tagged Photon Lab at Fermilab. This was necessary because the electrons in the M6 Meson Lab beam had a momentum spread larger than the calorimeter resolution. The points fall along the $20\%/\sqrt{E}$ line.

Fig. 10 shows a typical response to a 40 GeV beam. The muons cluster around 6 GeV while the rest of the beam shows a Gaussian peak at 40 GeV. The "t's" on the peak show the Gaussian fit. The hash mark on the abscissa marks 4σ from the peak mean; everything above 4σ is defined to be tail. The spectrum of Fig. 10 is typical in that the tail events are clearly separated from the Gaussian; the discussion of these events is not sensitive to where the cut is made.

To test the uniformity of response across the face of the calorimeter we moved the EM/FH unit horizontally and vertically across the beam. The horizontal scan shows no effects of the vertical cracks between scintillator pieces. The vertical scan does show effects of the horizontal cracks containing the wavebars. There are three separate effects: a peak shift, a peak broadening, and a peak tail.

Fig. 11 shows how the peak shifts and broadens as the beam crosses the wavebars. The peak mean varies by $\pm 5\%$ over the calorimeter face, while the resolution goes from $\pm 9\%$ away from the wavebars to $\pm 13\%$ at the wavebars. Fig. 12 shows the increase in the number of tail events at the wavebars. The

beam rate (5×10^4 /sec) times the gate width (100 nsec) gives an expected background accidental rate of 0.5%. At the wavebars there is an additional, roughly equal, component, due presumably to the direct particle/wavebar signal.

The 'straight-on' calibrating beam used in these tests greatly exaggerates the tail effect at the wavebars (Fig. 13). The calibrating beam puts particles right down the full length ($\sim 1\text{m}$) of the wavebar, and total internal reflection traps all the \checkmark C cone until it is shifted by the BBQ. A particle coming from the target during data taking cannot go down a wavebar because no wavebar plane contains the beam (Fig. 4). What does happen is that shower particles transit wavebars while leaking from one module to another. In this case particles traverse only 3mm, and they do it at angles steep enough that a substantial fraction ($\sim 20\%$) of the \checkmark C light exits before being shifted. To estimate the extent of this nonuniformity we compared the signals from the top and bottom neighbors of modules being calibrated (Fig. 13). The leakage signal from the top neighbor equals the leakage signal from the bottom neighbor plus the direct particle/wavebar signal generated by the top neighbor's wavebar. The data show no difference between the two leakage signals, indicating that this nonuniformity is negligible.

Even if the 'worst case' calibrating beam results are taken as indicative of operational conditions, the calorimeter is still adequately uniform. Those results imply that over a very small area ($\sim 2\%$) there is a very small probability ($\sim 1\%$)

of a particle energy being boosted; the limit on the boost is 60%. Even at that, the high multiplicity of high- P_t events washes out the effect of any one particle being boosted. A preliminary look at our high- P_t data sample sees no sign of any nonuniformities.

ACKNOWLEDGEMENT

We wish to express appreciation for the supporting efforts of the Fermilab E557 collaboration: Fermilab, University of Illinois (Chicago Circle), Indiana University, University of Maryland, and Rutgers University.

In addition we would like to thank several Fermilab people for their excellent technical contributions. They are Jack Doskow, Pat Gorak, Bruce Hanna, Dean Lee, and Carl Lindenmeyer.

References

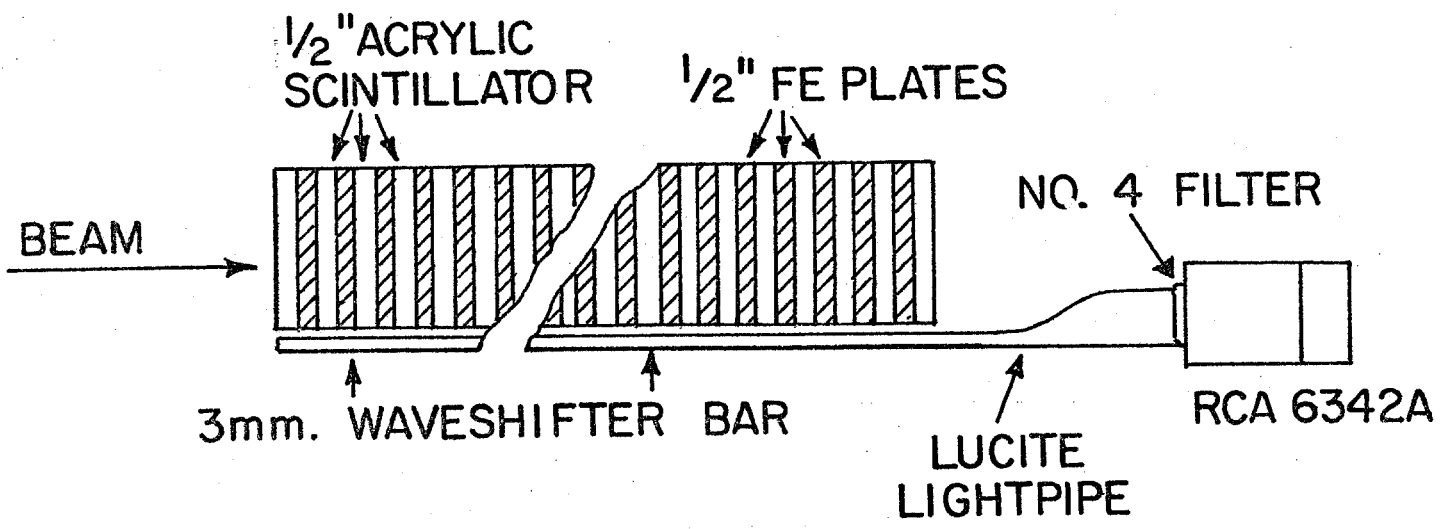
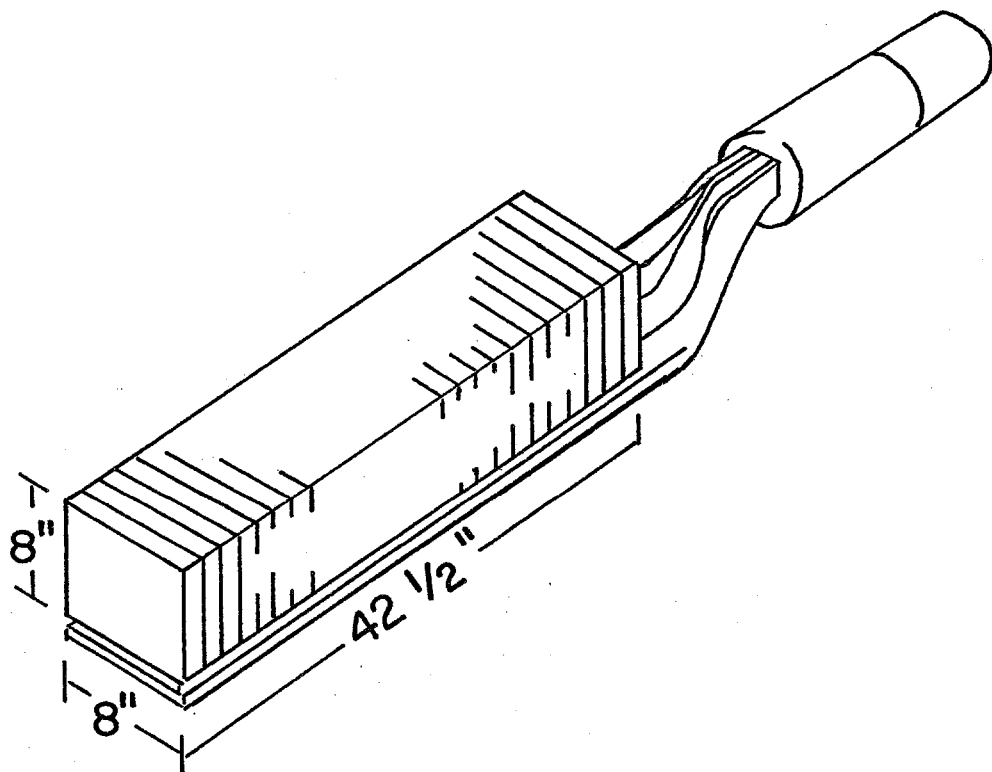
1. A. Erwin, E. Harvey, A. Kanofsky, W. Kononenko, T. Kondo, L. Kroger, R. Loveless, W. Selove, F. Turkot, D. Winn, B. Yost, Proceedings of the Calorimeter Workshop (Fermilab, 1975) p. 271.
2. W.B. Atwood, C.Y. Prescott, L.S. Rochester, B.C. Barish, SLAC-TN-76-7 (Dec. 1976).
3. W.A. Shurcliff, J. Opt. Soc. Am. 41 (1951) 209.
R.L. Garwin, Rev. Sci. Instr. 31 (1960) 1010.
G. Keil, Nucl. Instr. and Meth. 87 (1970) 111.
4. W. Kienzle, G. Matthiae, R. Vanderhagen, S. Weisz, G. Burgun, Scintillator Developments at CERN (NP Internal Report 75-12, CERN, Oct. 1975).
5. V. Eckardt, R. Kalbach, A. Manz, K.P. Pretzl, N. Schmitz, D. Vranic, A Novel Light Collection System for Segmented Scintillation Counter Calorimeters (MPI-PAE/Exp.E1.70, Max-Planck-Institut, April 1978).
6. The scintillator was supplied by Polytech, Inc. of Owensville, Missouri.
7. The wavebars were supplied by Rohm of Darmstadt, West Germany. Their name for the material is Rohaglas GS2029.
8. TiO_2 paint from the local hardware store tested to be more reflective than Nuclear Enterprise's TiO_2 paint.
9. Alzac is a polishing process of Alcoa. It produces a specular reflectivity of approximately 65%.

Table 1. Calorimeter Depth

UNIT	MATERIAL	RADIATION LENGTHS	ABSORPTION LENGTHS
EM	14x1/4" Pb	15.9	0.48
	15x1/2" Sc	<u>0.6</u>	<u>0.29</u>
		16.4	0.77
FH	40x1/2" Fe	28.9	2.97
	40x1/2" Sc	<u>1.5</u>	<u>0.78</u>
		30.3	3.75
BH	22x1" Fe	31.8	3.27
	22x1/2" Sc	<u>0.8</u>	<u>0.43</u>
		32.6	3.70
		79.3	8.22

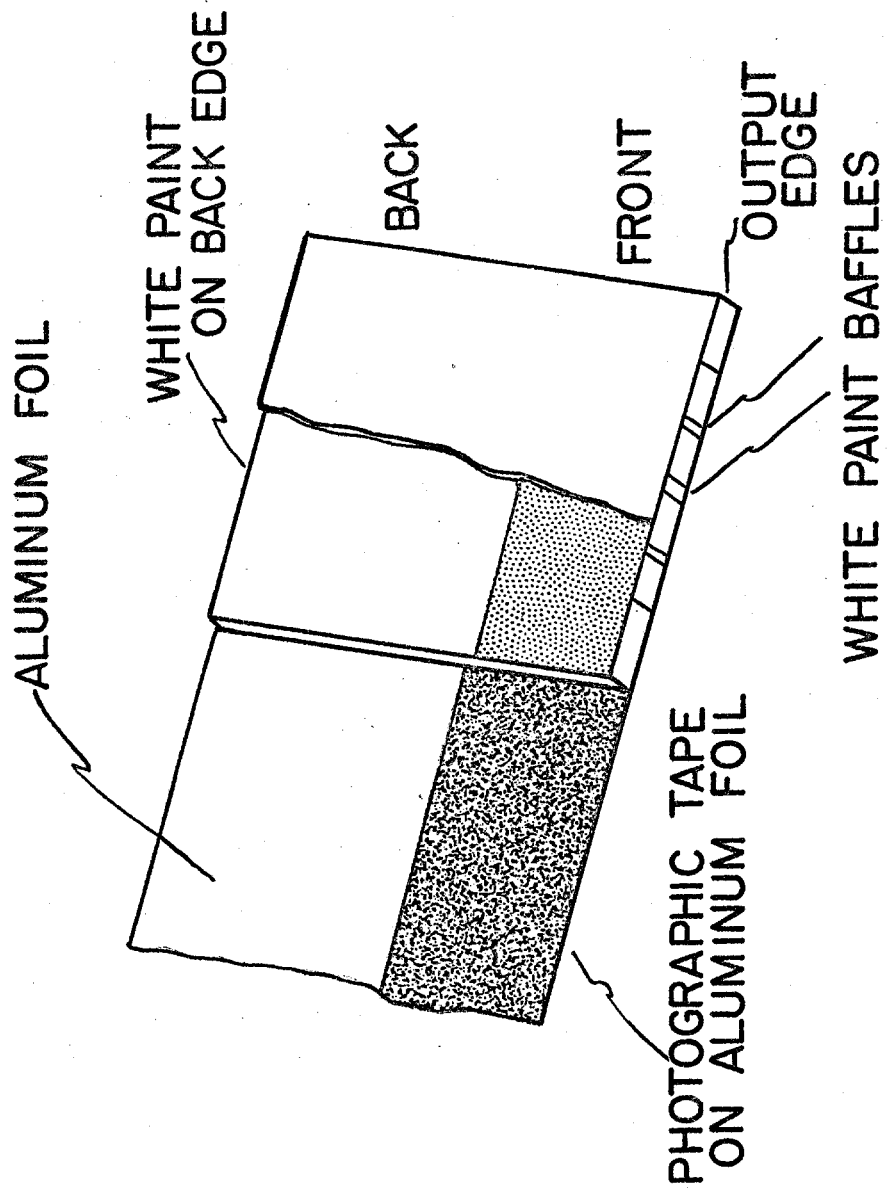
FIGURES

1. Basic Shower Module
2. Scintillator Wrapping and Masking
3. Exploded View of Module Construction
4. EM/FH Crate Stacking
5. EM/FH Modularity
6. BH Modularity
7. Linearity
8. Hadron Resolution
9. Electron Resolution
10. Response to 40 GeV Beam
11. Peak Shifting and Broadening at Wavebars
12. Gaussian Tail at Wavebars
13. Calibration Beam as Worst Case Effect at Wavebars



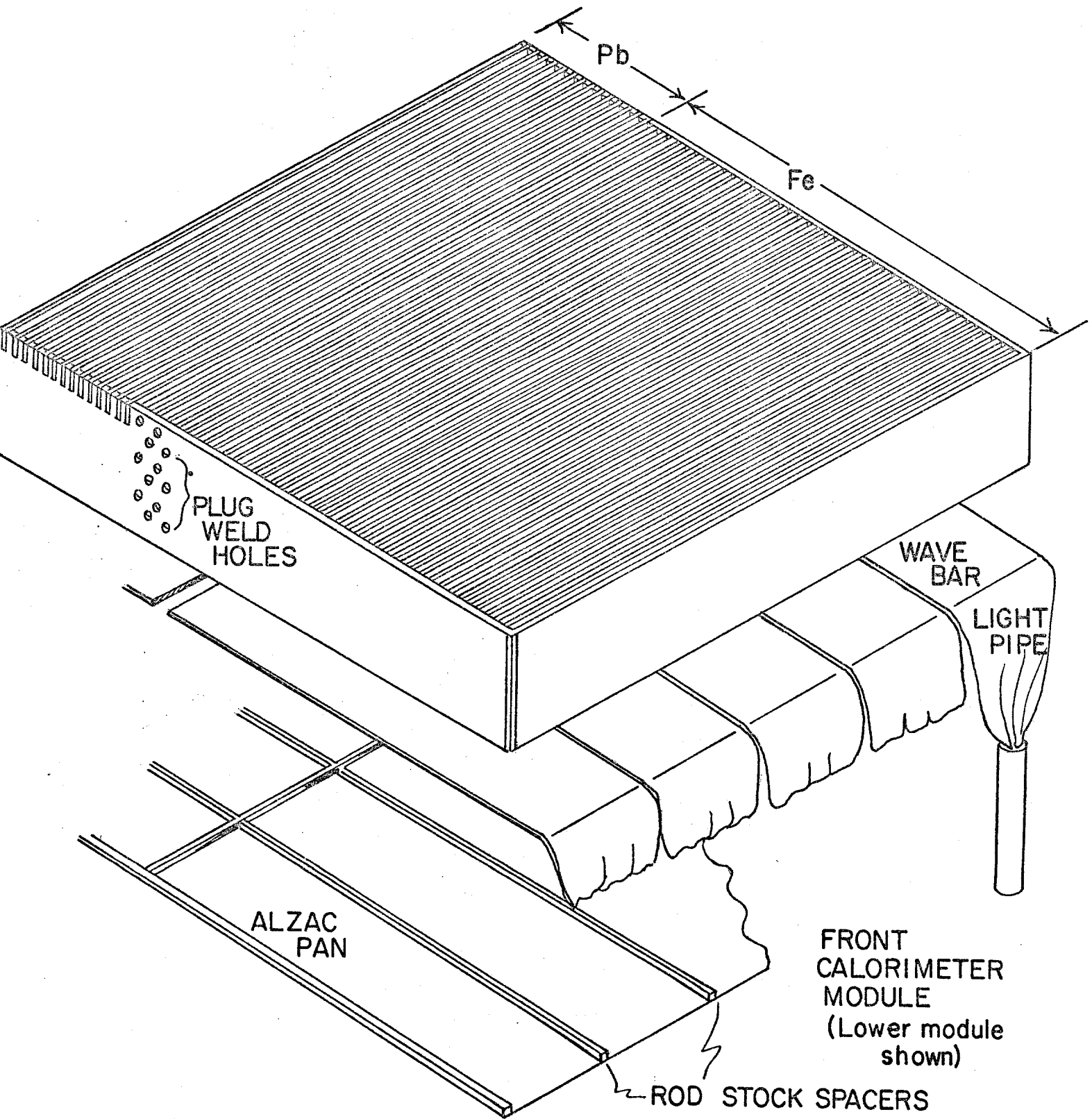
FRONT HADRON MODULE
(curved lightpipe not shown)

Fig. 1



SCINTILLATOR WRAPPING AND MASKING

Fig. 2



MODULE CONSTRUCTION

Fig. 3

EM/FH STACK

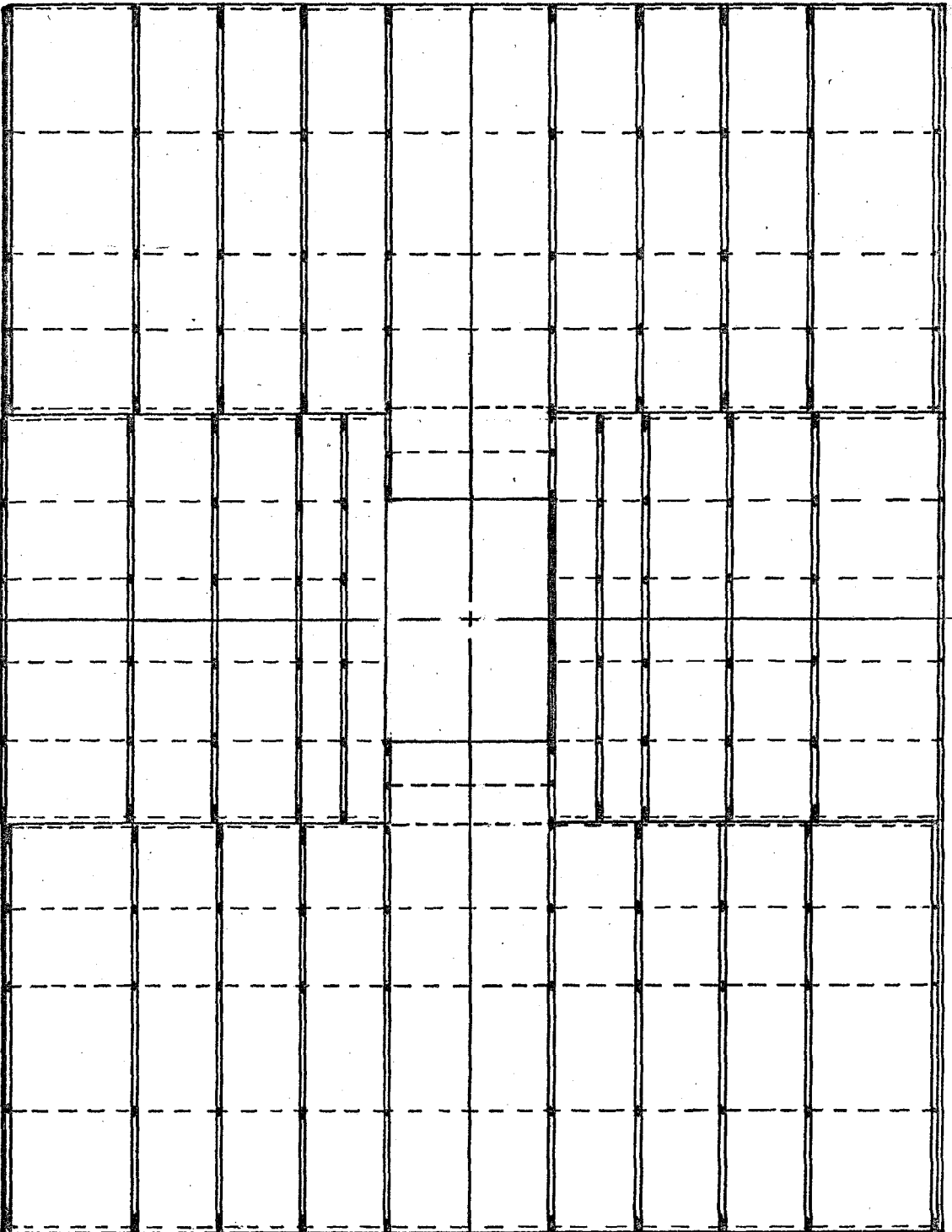
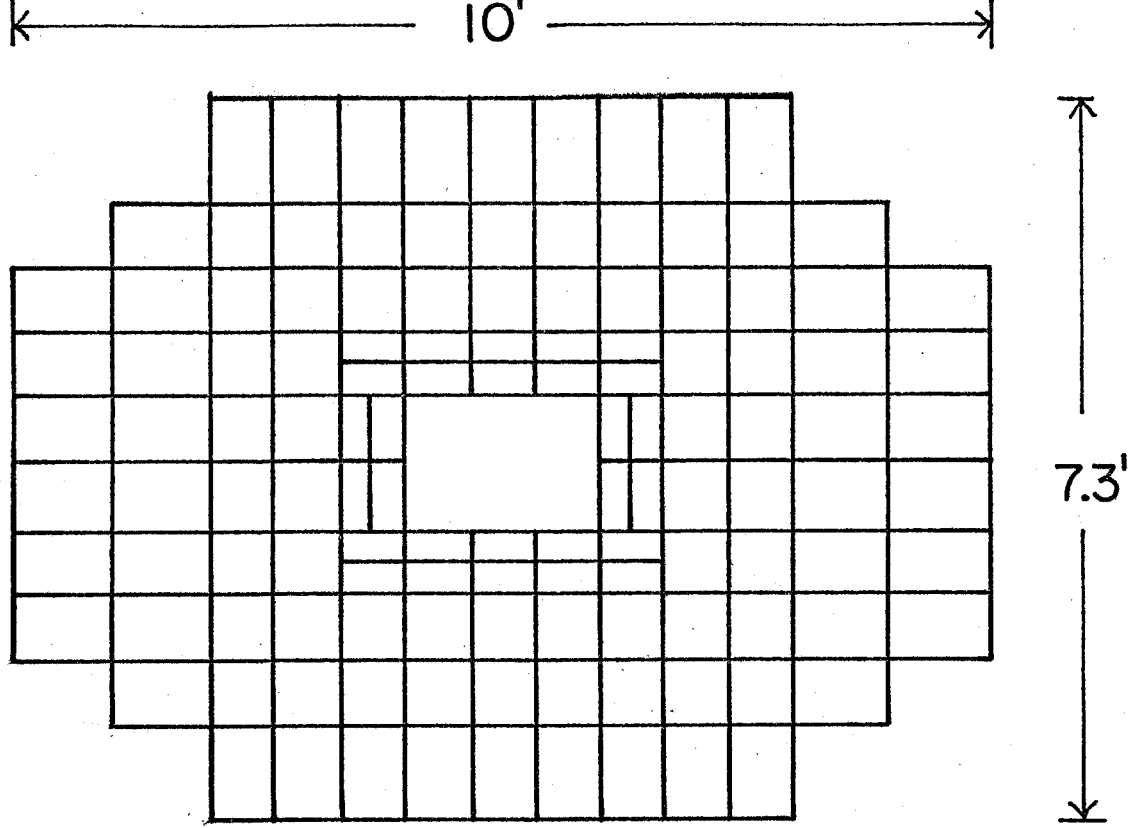
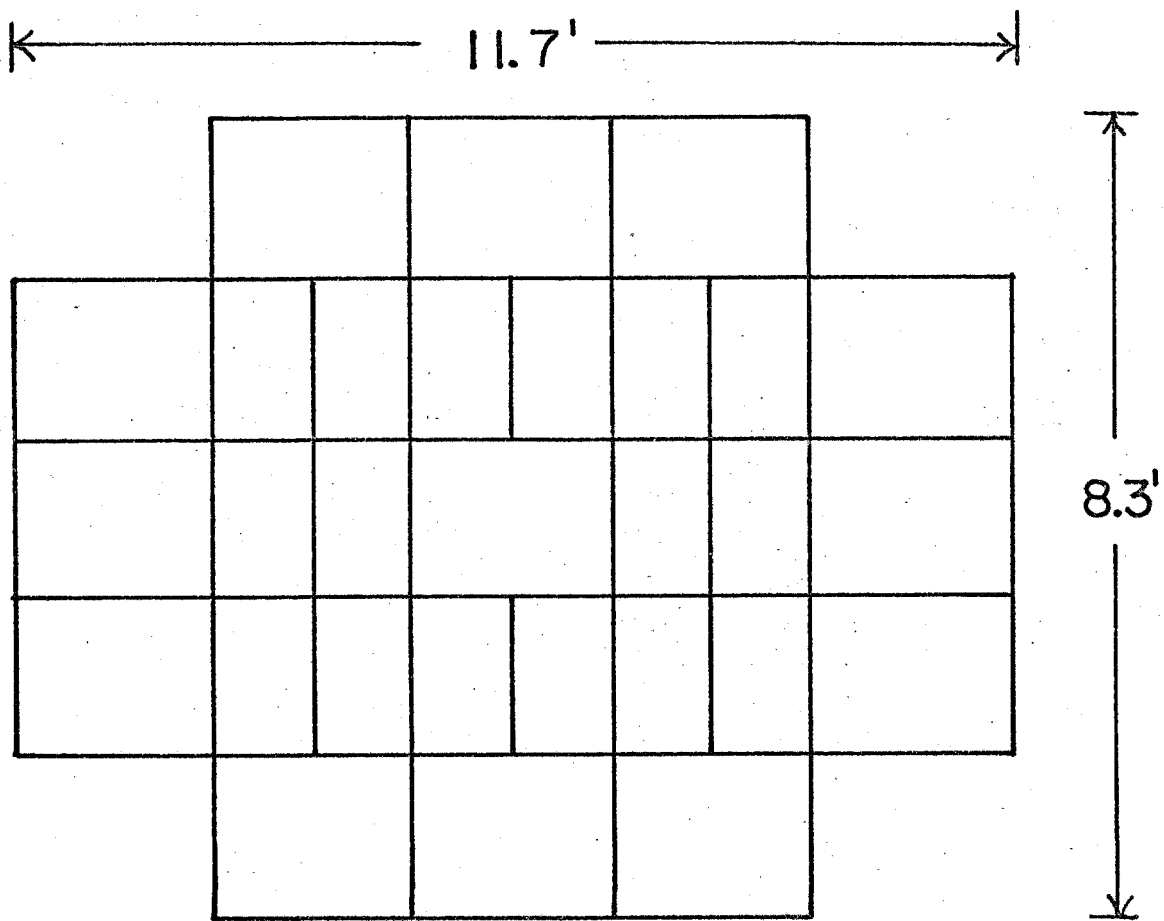


Fig. 4



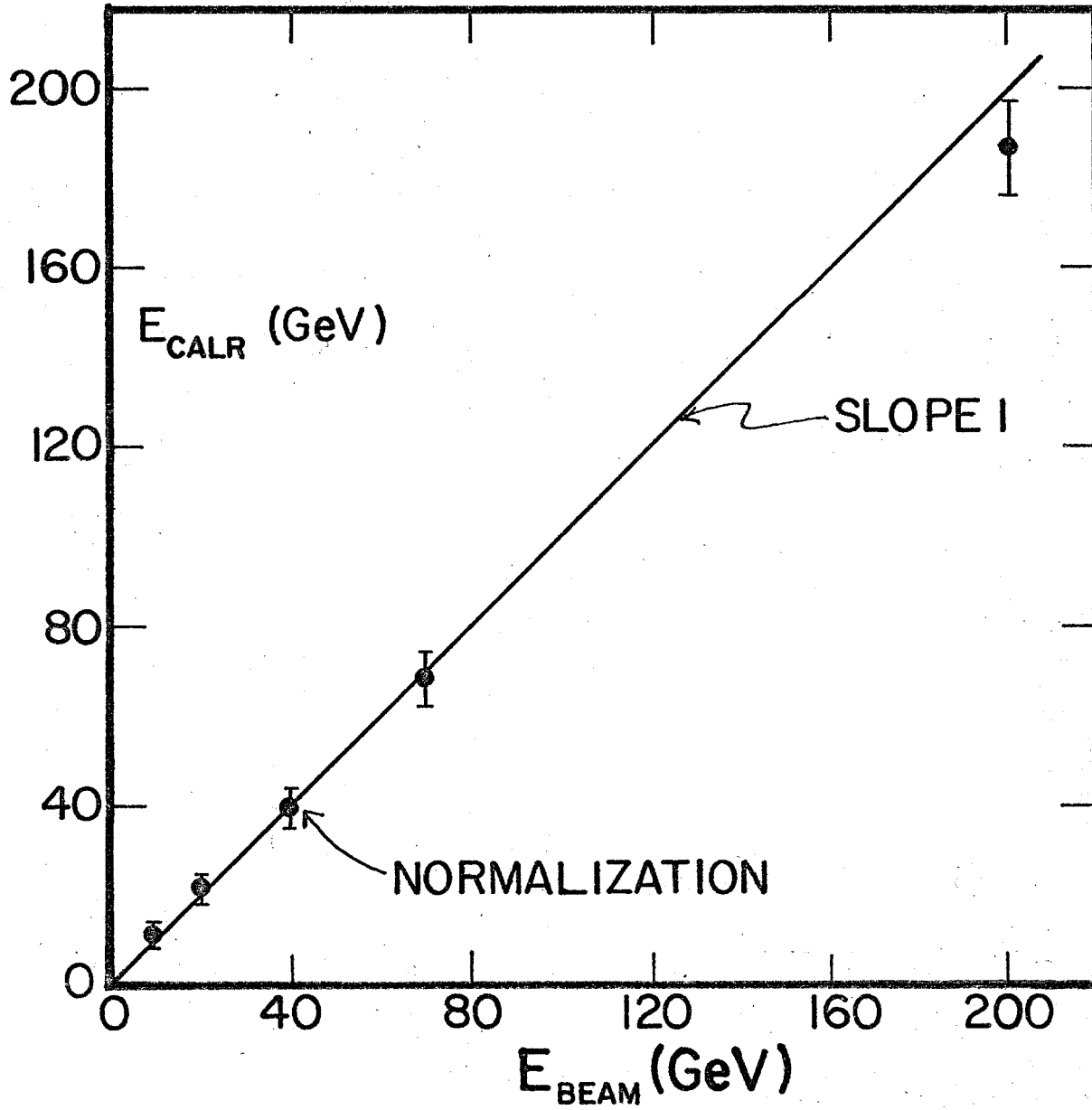
EM/FH MODULARITY

Fig.5



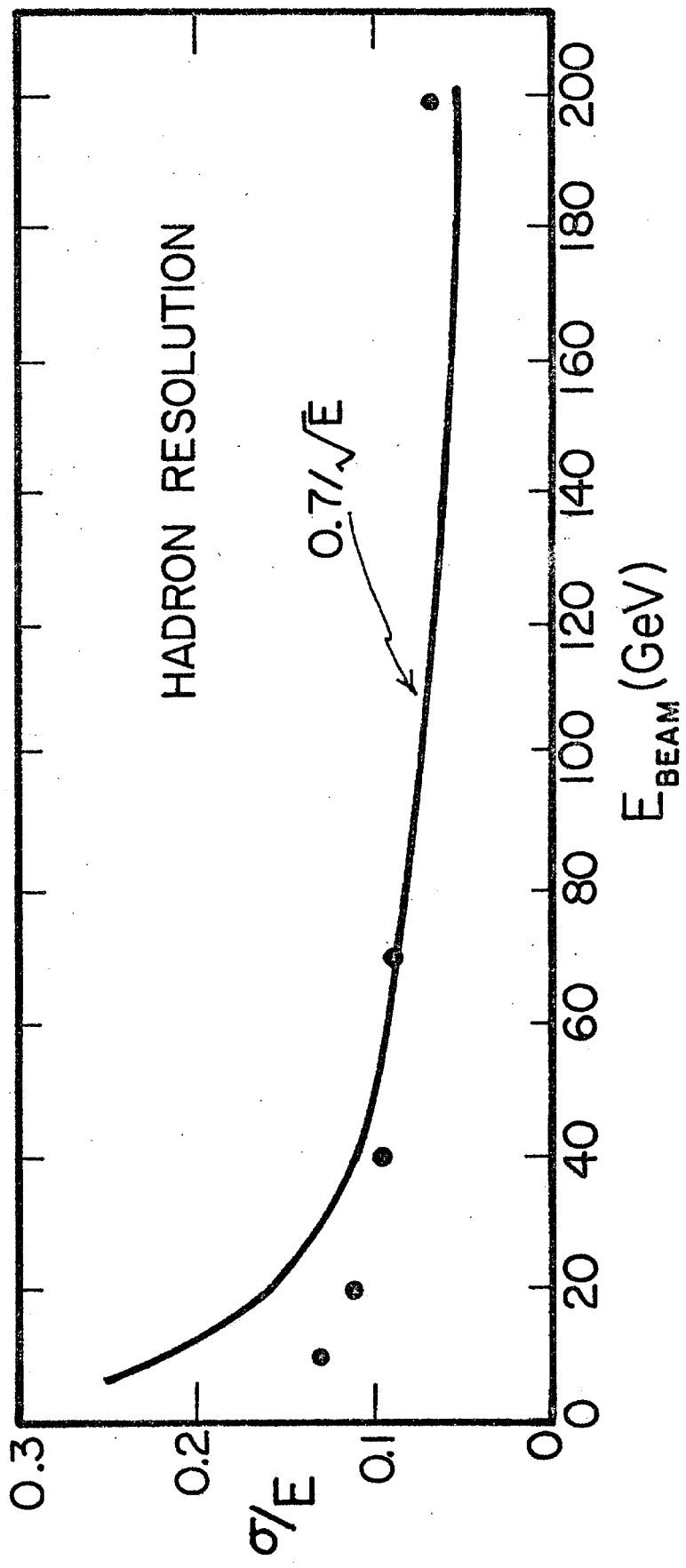
BH MODULARITY

Fig.6



LINEARITY

Fig.7



HADRON RESOLUTION
Fig. 8

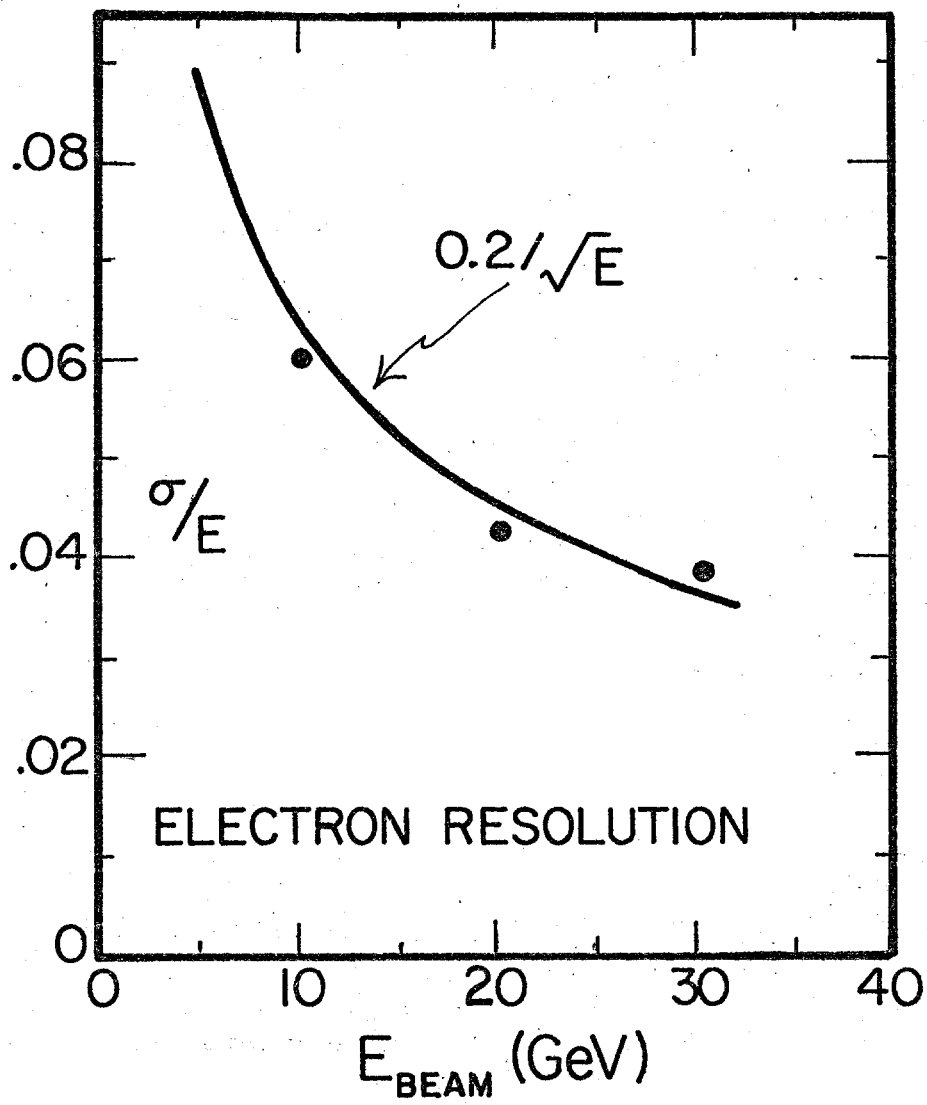


Fig. 9

ARBITRARY SCALE

40 GeV

FITTED
GAUSSIAN

E_{CALR} (GeV)

0 10 20 30 40 50 60 70 80

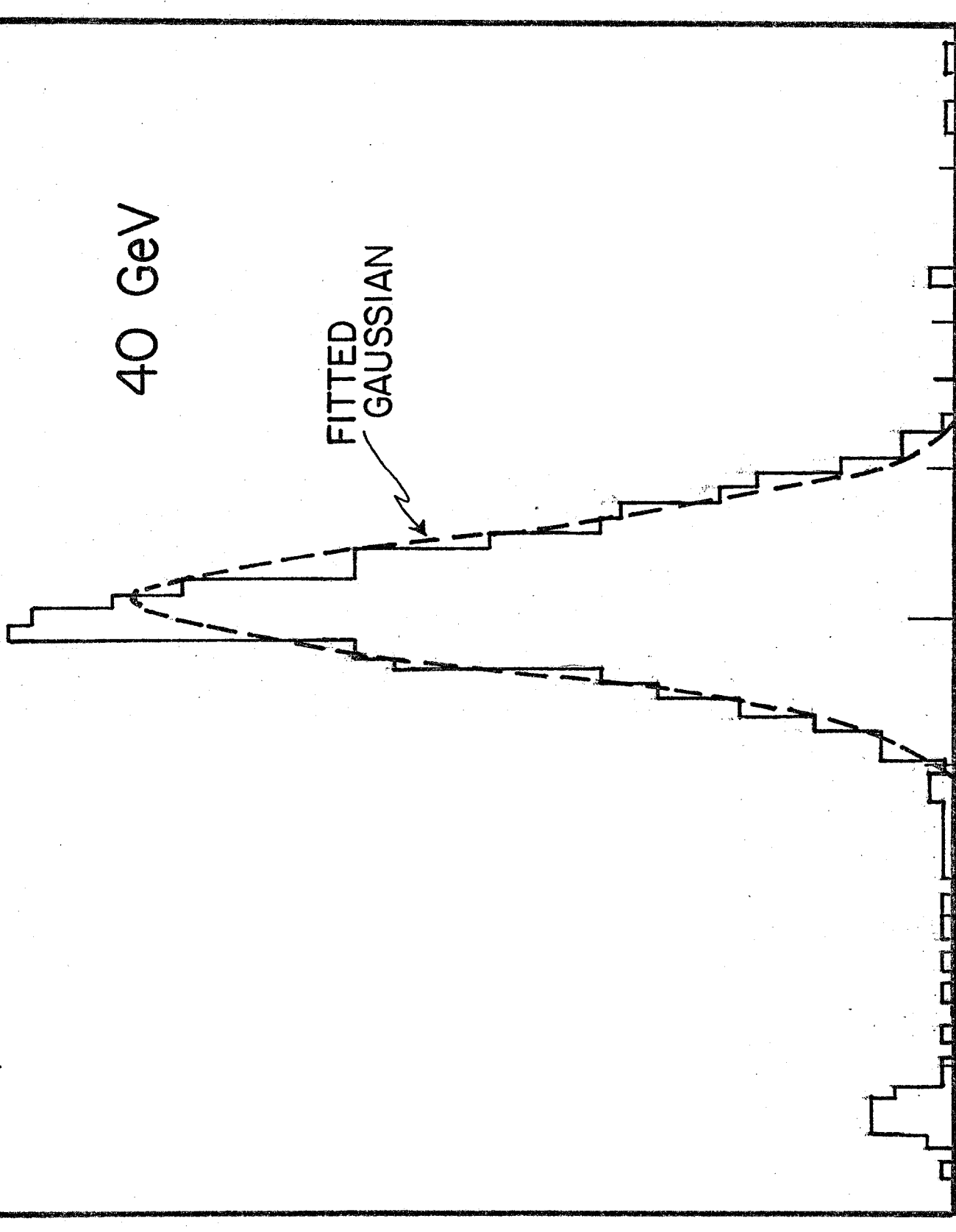


Fig. 10

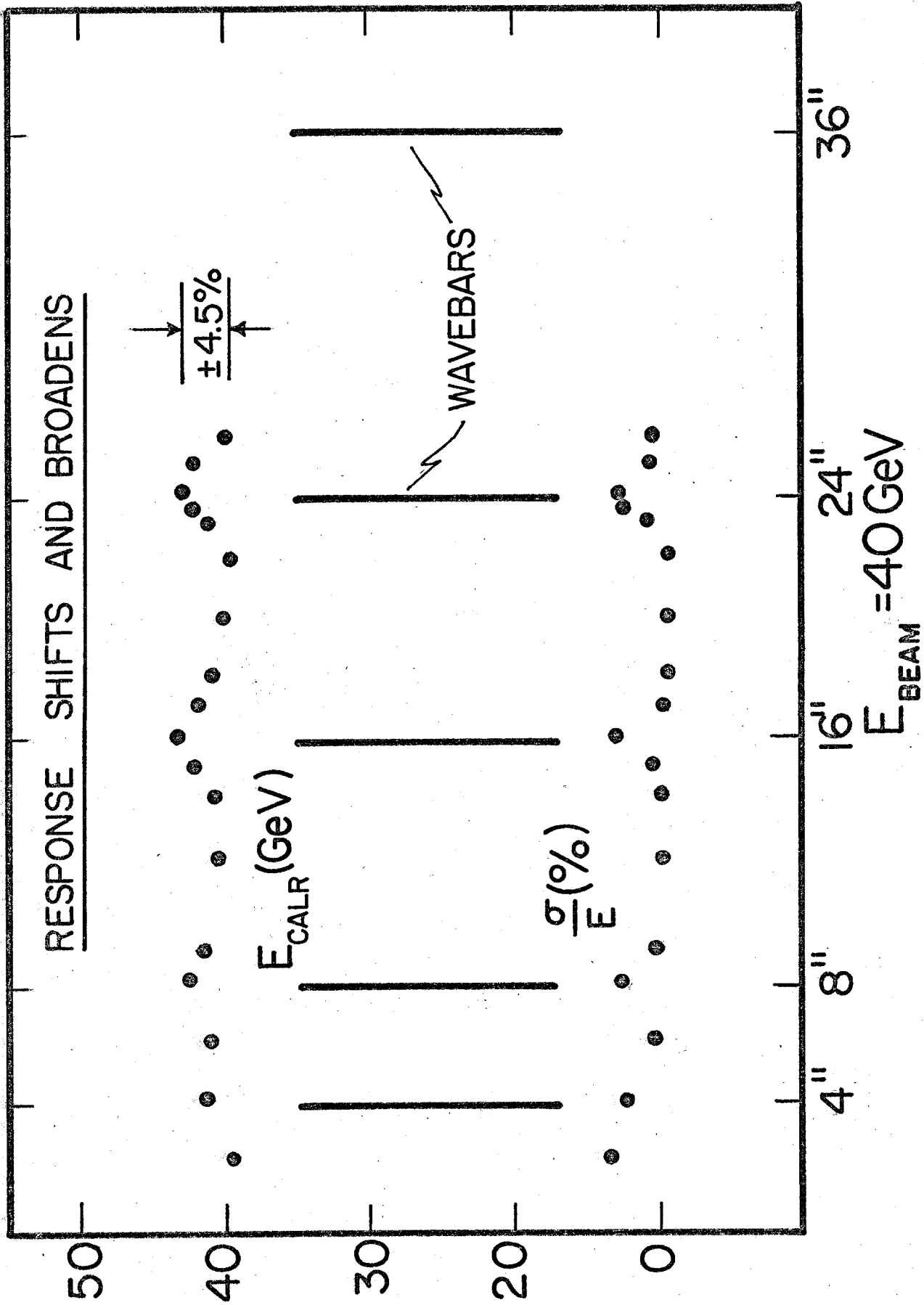


Fig. II

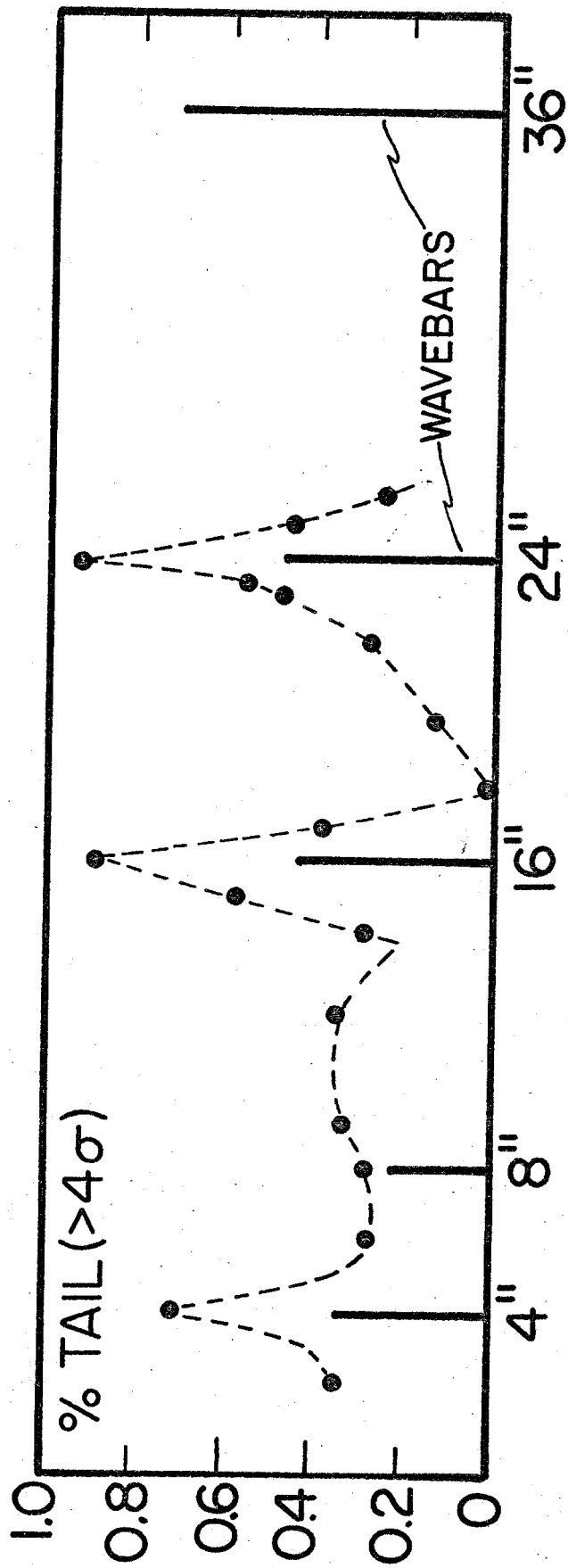


Fig. 12

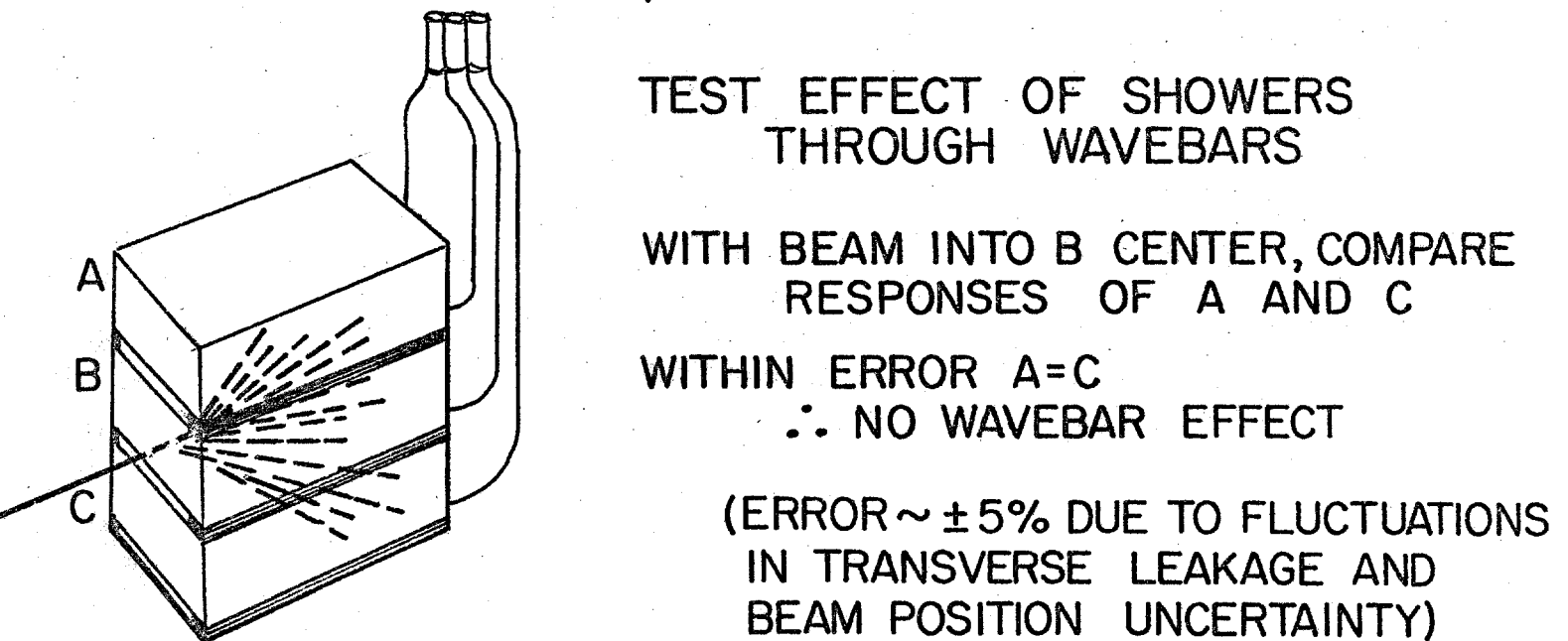
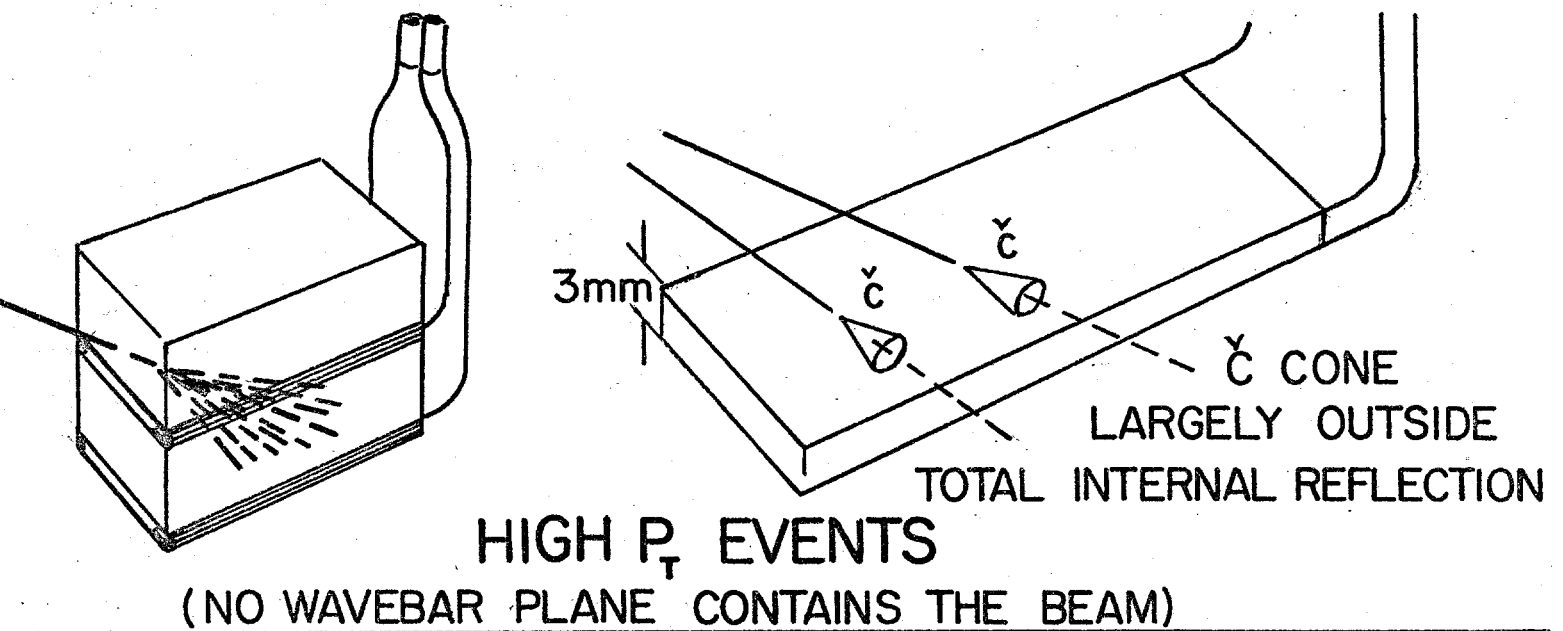
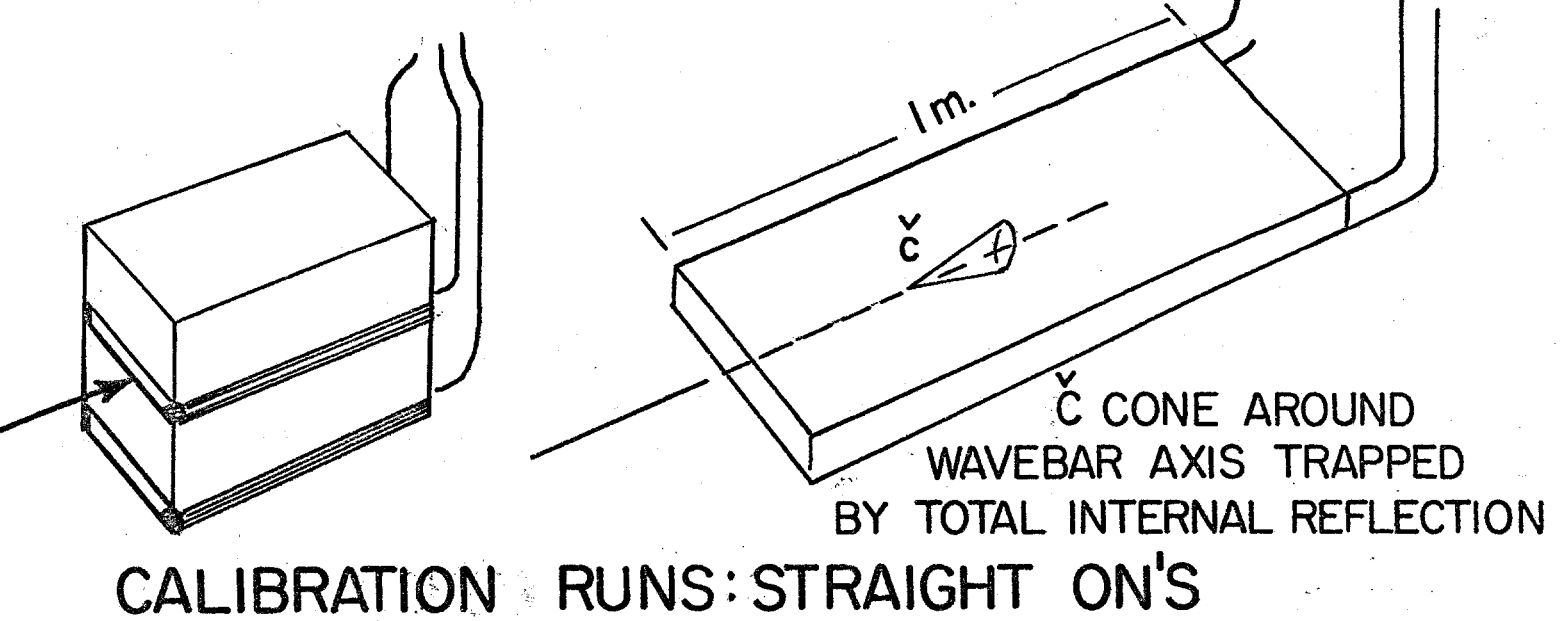


Fig. 13